



# High-Order Residual Distribution Schemes for Steady 1D Relativistic Hydrodynamics

James A. Rossmannith

**ABSTRACT.** An important goal in astrophysics is to model phenomena such as the gravitational collapse of stars and accretion onto black holes. Under the assumption that the spacetime metric remains fixed on the time scales of fluid motion, the relevant physics can be modeled by the equations of relativistic hydrodynamics. These equations form a system of hyperbolic balance laws that are strongly nonlinear and exhibit shock formation. In recent years several types of numerical methods have been developed for relativistic hydrodynamics; perhaps the most successful have been high-resolution shock-capturing schemes based either on Godunov, ENO, or central schemes. We present in this work some preliminary results on an alternative approach based on residual distribution schemes. The main attraction of these methods is that they can be made high-resolution shock-capturing and high-order accurate through the use of compact stencils. In the current work we focus specifically on developing second, fourth, and sixth-order accurate residual distribution schemes for 1D steady flows.

## 1. Introduction

Astrophysics, much like weather prediction and climatology, is a field of science in which observations are possible, but direct experimentation is not. Therefore, direct experiments are replaced by computer simulations. In particular, theoretical astrophysics is concerned with understanding phenomena such as the dynamics of interacting black holes, the gravitational collapse of massive stars, the accretion of matter onto black holes, and the evolution of binary neutron stars. The governing equations for these phenomena are the Einstein equations, which couple the dynamics of spacetime to the dynamics of matter. These equations are strongly nonlinear and solutions can become singular through the formation of shockwaves and geometric singularities [7].

In order to overcome these difficulties, several types of numerical methods have been developed including finite difference, pseudo-spectral, and smoothed-particle hydrodynamic methods. Although these methods each have their own advantages, perhaps the class of methods that has received the most attention in recent years is that of high-resolution shock-capturing schemes such as those based on Godunov, ENO (essentially non-oscillatory), and central schemes (see Font [6] for a detailed review of these approaches).

In this work, we present some preliminary results on an alternative to the high-resolution schemes currently in use in the astrophysics community. We consider a class of methods known as residual distribution schemes, which are based on a truly multi-dimensional extension of the scalar upwind scheme (see Abgrall [1] for a review). The method is naturally formulated on triangular grids, making it an ideal approach for flows in complex geometries. Several improvements to the schemes discussed in [1] have been proposed in recent years such as the development of second-order accurate monotone schemes for unsteady flows [2, 4], and high-order methods for steady scalar equations [3]. Further development is still an area of active research.

In this paper we develop a high-order residual method for steady 1D relativistic hydrodynamics. The proposed method makes use of the approach developed by [3] and extends it to 1D systems of hyperbolic balance laws. This scheme is described in Section 3 and tested on a special and a general relativistic numerical example in Section 4.

## 2. Relativistic Hydrodynamics

The general theory of relativity is described mathematically by the Einstein equations [7]:

$$(1) \quad R^{\mu\nu} - \frac{1}{2}Rg^{\mu\nu} = 8\pi T^{\mu\nu},$$

where  $\mu$  and  $\nu$  are indices that range from 0 to 3,  $g^{\mu\nu}$  is the inverse metric tensor,  $R^{\mu\nu}$  is the Ricci curvature tensor,  $R$  is the scalar curvature, and  $T^{\mu\nu}$  is the energy-momentum tensor. These equations couple the dynamics of matter (the right-hand side of (1)) to the evolution of the spacetime metric (the left-hand side of (1)). In some applications such as in the accretion of matter onto black holes, the background spacetime geometry changes very little on the times-scales of the fluid motion. In such a situation the *test-fluid approximation* is invoked, which renders the spacetime geometry fixed and reduces the Einstein equations to the *relativistic hydrodynamic* equations:

$$(2) \quad \nabla_{\mu}T^{\mu\nu} = 0,$$

$$(3) \quad \nabla_{\mu}J^{\mu} = 0,$$

where the application of  $\nabla_{\mu}$  implies covariant differentiation,  $J^{\mu}$  is the matter current density, and equation (3) is the continuity equation.

A typical assumption is to make the fluid an ideal gas with gas constant  $\Gamma$ . This results in the following form of the energy-momentum tensor and the matter current density [6]:

$$(4) \quad T^{\mu\lambda} = \rho h v^\mu v^\lambda W^2 + p g^{\mu\lambda},$$

$$(5) \quad J^\mu = \rho W v^\mu.$$

Here  $\rho$  is the fluid density,  $v^\mu = (1, v^1, v^2, v^3)$  is the fluid velocity,  $p$  is the pressure,

$$(6) \quad h = 1 + \frac{p\Gamma}{\rho(\Gamma - 1)}$$

is the specific relativistic enthalpy, and

$$(7) \quad W = (-g_{00} - 2g_{0i}v^i - g_{ij}v^i v^j)^{-1/2}$$

is the Lorentz factor. The Lorentz factor lies between  $W = 1$  (the Newtonian limit) and  $W = \infty$  (the ultra-relativistic limit) and measures how close the fluid speed is to the speed of light ( $c = 1$ ).

## 2.1. Covariant formulation of relativistic hydrodynamics

One difficulty with the Einstein equations is that there exist several ways to formulate the equations as an initial value problem. The most commonly used is the 3+1 ADM formulation, in which spacetime is foliated into spacelike hypersurfaces. However, as is pointed by Font [6], in the framework of high-resolution shock-capturing schemes a covariant formulation may be more natural. For this reason we make use of the covariant formulation described in [8], which yields the following hyperbolic system:

$$(8) \quad \frac{\partial}{\partial x^0} \left( \sqrt{-g} \begin{bmatrix} D \\ S^j \\ E \end{bmatrix} \right) + \frac{\partial}{\partial x^i} \left( \sqrt{-g} \begin{bmatrix} \rho v^i W \\ \rho h v^i v^j W^2 + p g^{ij} \\ \rho h v^i W^2 + p g^{i0} \end{bmatrix} \right) = \psi,$$

where  $\psi = (0, -\sqrt{-g} \Gamma_{\mu\lambda}^i T^{\mu\lambda}, -\sqrt{-g} \Gamma_{\mu\lambda}^0 T^{\mu\lambda})$  is a geometric source term,  $\sqrt{-g}$  is the square root of the determinant of the metric tensor,  $D$  is the rest mass,  $S = (S^1, S^2, S^3)$  is the fluid momentum, and  $E$  is the fluid energy. The  $\Gamma_{\mu\lambda}^\nu$ 's that appear in the source term are called *Christoffel symbols* or *connection coefficients* and can be computed by taking first-order derivatives of the metric tensor [7]. Finally, the conserved variables are related to the primitive variables through the following nonlinear relationship:

$$(9) \quad \begin{bmatrix} D \\ S^j \\ E \end{bmatrix} = \begin{bmatrix} \rho W \\ \rho h v^j W^2 + p g^{0j} \\ \rho h W^2 + p g^{00} \end{bmatrix}.$$

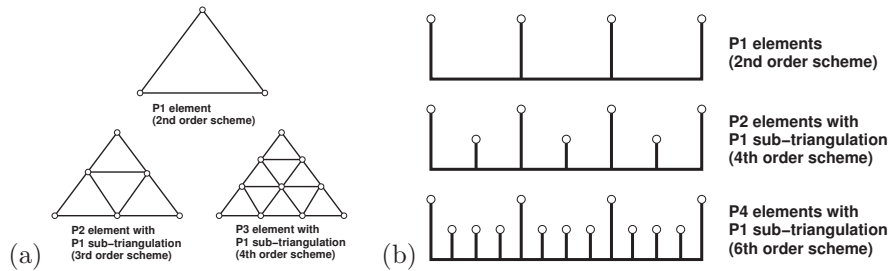


FIGURE 1. High-order elements in (a) two-space dimensions as proposed by Abgrall and Roe [3] and in (b) one-space dimension. In 1D using either  $P^{2n}$  or  $P^{2n+1}$  elements produces schemes that have a theoretical order of accuracy of  $2n + 2$ .

## 2.2. Foliations of spacetime

An advantage of the covariant formulation is that one is free to choose either a spacelike or a null foliation of spacetime. Spacelike foliations are the most natural, but require a Newton iteration in the recovery of the primitive variables from the conserved variables. An efficient way to handle this is to write a single equation for  $W$ , solve using a Newton iteration, and then use this result to directly evaluate the primitive variables (see for example [9]). Alternatively, in some cases it may be advantageous to choose a null foliation (i.e.,  $g^{00} \equiv 0$ ), in which case the primitive variables can be directly recovered from the conserved variables [8]. In the numerical examples we will test both of these approaches.

## 3. Residual Distribution Schemes for 1D Balance Laws

We develop in this section a second and a fourth order residual distribution scheme for 1D balance laws. Furthermore, in this description we show how one can generalize these results to obtain any desired order of accuracy.

### 3.1. A monotone and linear-preserving scheme

Consider a 1D balance law of the form:

$$(10) \quad \frac{\partial}{\partial t}(\kappa q) + \frac{\partial}{\partial x} f(q, x) = \psi(q, x),$$

where  $q, f, \psi \in \mathbb{R}^m$  are the vectors denoting the conserved variables, flux function, and source term, respectively.  $\kappa(x)$  is a capacity function, which in the case of relativistic hydrodynamics is  $\sqrt{-g}$ .

We construct a mesh that consists of  $N$  elements,  $\mathcal{T}_i$ , which lie between nodes  $x = x_i$  and  $x = x_{i+1}$ . On each node at each time level, we define an approximate

solution:  $Q_i^n \approx q(x_i, t^n)$ . The exact total residual in element  $\mathcal{T}_i$  is given by

$$(11) \quad \Phi^{\mathcal{T}_i} = \int_{x_i}^{x_{i+1}} (f_x(q, x) - \psi(q, x)) dx = f_{i+1} - f_i - \int_{x_i}^{x_{i+1}} \psi(q, x) dx.$$

This integral can be approximated to second order using the trapezoidal rule:

$$(12) \quad \phi^{\mathcal{T}_i} = f_{i+1} - f_i - \frac{\Delta x}{2} (\psi_{i+1} + \psi_i).$$

A linear-preserving and monotone residual distribution scheme is obtained by distributing  $\phi^{\mathcal{T}_i}$  to nodes  $i$  and  $i + 1$  based on the eigenvalues of

$$(13) \quad \hat{A} = \frac{\partial f}{\partial q} \left( \frac{1}{2} (Q_i^n + Q_{i+1}^n) \right).$$

The full numerical update is given by

$$(14) \quad Q_i^{n+1} = Q_i^n - \frac{\Delta t}{\kappa_i \Delta x} (\phi_+^{\mathcal{T}_{i-1}} + \phi_-^{\mathcal{T}_i}),$$

$$(15) \quad \phi_+^{\mathcal{T}_i} = \sum_{p: \hat{s}^p > 0} \hat{\ell}^p \cdot \phi^{\mathcal{T}_i} \hat{r}^p + \frac{1}{2} \sum_{p: \hat{s}^p = 0} \hat{\ell}^p \cdot \phi^{\mathcal{T}_i} \hat{r}^p,$$

$$(16) \quad \phi_-^{\mathcal{T}_i} = \sum_{p: \hat{s}^p < 0} \hat{\ell}^p \cdot \phi^{\mathcal{T}_i} \hat{r}^p + \frac{1}{2} \sum_{p: \hat{s}^p = 0} \hat{\ell}^p \cdot \phi^{\mathcal{T}_i} \hat{r}^p,$$

where  $\hat{s}^p$ ,  $\hat{r}^p$ , and  $\hat{\ell}^p$  are the  $p^{\text{th}}$  eigenvalue, right eigenvector, and left eigenvector of  $\hat{A}$ , respectively. Note that  $\phi^{\mathcal{T}_i} = \phi_+^{\mathcal{T}_i} + \phi_-^{\mathcal{T}_i}$  by construction, which ensures that this scheme is numerically conservative. This scheme is equivalent to the first order in time scheme proposed in [5].

### 3.2. High-order extensions

The scheme presented above is second order accurate in the steady-state because the residual is  $\phi^{\mathcal{T}_i} = \mathcal{O}(\Delta x^3)$ . In order to improve the accuracy, integral (11) must be approximated to higher accuracy. In order to maintain a compact stencil, Abgrall and Roe [3] introduce additional points by subdividing element  $T_i$  into sub-elements (see Figure 1).

For example, the scheme described above can be improved by adding an additional node at the point  $x_{i+\frac{1}{2}}$ , allowing us to interpolate  $\psi$  in element  $\mathcal{T}_i$  with a quadratic polynomial. Next we define two sub-residuals,  $\phi^{\mathcal{T}_{1,i}}$  and  $\phi^{\mathcal{T}_{2,i}}$ , by integrating the interpolated  $\psi$  from  $x_i$  to  $x_{i+\frac{1}{2}}$  and  $x_{i+\frac{1}{2}}$  to  $x_{i+1}$ , respectively. These sub-residuals are now distributed to nodes  $i$ ,  $i + \frac{1}{2}$ , and  $i + 1$  according to eigenstructure of  $\hat{A}$  in each sub-element. The resulting scheme can be summarized as follows:

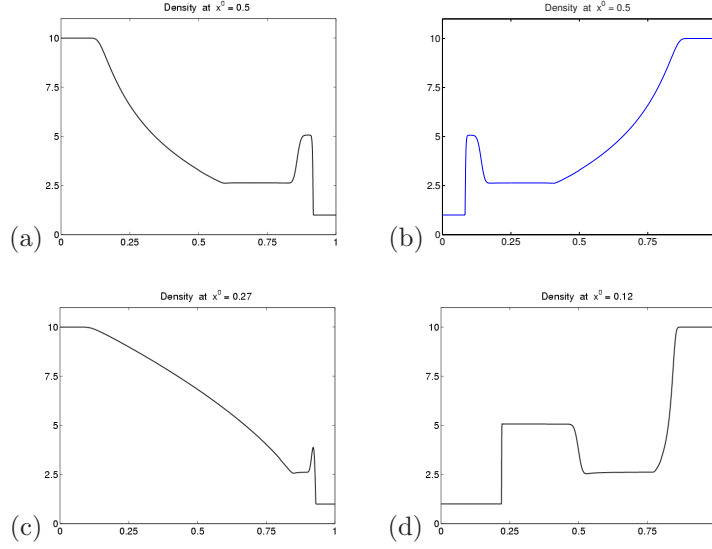


FIGURE 2. Solution to a special relativistic Riemann problem using the  $P^1$  residual distribution scheme with 2000 points.

$$\begin{aligned}\phi^{\mathcal{J}_{1,i}} &= f_{i+\frac{1}{2}} - f_i - \frac{\Delta x}{24} \left( 5\psi_i + 8\psi_{i+\frac{1}{2}} - \psi_{i+1} \right), \\ \phi^{\mathcal{J}_{2,i}} &= f_{i+1} - f_{i+\frac{1}{2}} - \frac{\Delta x}{24} \left( -\psi_i + 8\psi_{i+\frac{1}{2}} + 5\psi_{i+1} \right), \\ Q_i^{n+1} &= Q_i^n - \frac{\Delta t}{\kappa_i \Delta x} \left( \phi_+^{\mathcal{J}_{2,i-1}} + \phi_-^{\mathcal{J}_{1,i}} \right), \\ Q_{i+\frac{1}{2}}^{n+1} &= Q_{i+\frac{1}{2}}^n - \frac{\Delta t}{\kappa_{i+\frac{1}{2}} \Delta x} \left( \phi_+^{\mathcal{J}_{1,i}} + \phi_-^{\mathcal{J}_{2,i}} \right),\end{aligned}$$

where  $Q_{i+\frac{1}{2}}$  denotes the solution in the center of element  $\mathcal{J}$ . This scheme is in fact fourth order accurate, since  $\phi^{\mathcal{J}_{1,i}} + \phi^{\mathcal{J}_{2,i}} = \mathcal{O}(\Delta x^5)$  by Simpson's rule. Finally, a sixth order scheme can be obtained by subdividing each element  $\mathcal{J}$  into four sub-elements. We omit the formulas for this scheme.

## 4. Numerical Examples

The residual distribution schemes developed in the previous section are applied to two test cases proposed by Papadopolous and Font [8].

### 4.1. A special relativistic Riemann problem

Although the schemes considered here are only first order accurate in time, we apply them to a special relativistic Riemann problem in order to demonstrate the

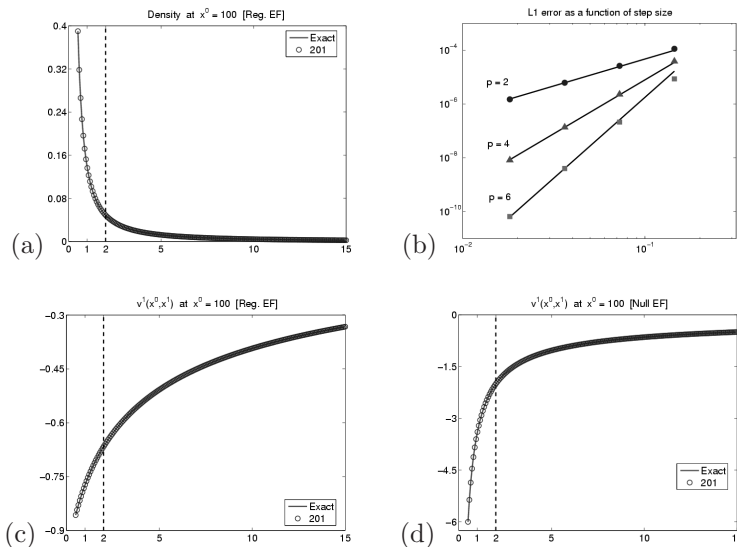


FIGURE 3. Steady-state solution of dust accretion onto a Schwarzschild black hole.

shock-capturing ability of the scheme and to investigate the differences between spacelike and null foliations of spacetime. Special relativity is described by the Minkowski metric, which represents a spacelike foliation. A null foliation can be obtained through the change of variables  $v = x + t$ . The Minkowski metric and its null coordinate counterpart can be written as

$$(17) \quad ds^2 = -dt^2 + dx^2 \quad \text{and} \quad ds^2 = -dv^2 + 2dx dv,$$

respectively.

The solution to a Riemann problem in the standard Minkowski coordinates is shown in Figure 2(a). In Figure 2(b) the same problem is solved but with the initial left and right states interchanged. Plots (c) and (d) show the solution in the null coordinates; in these plots the left-half of the plot is in the relative future compared to the right-half. Therefore, in Figure 2(c) the rarefaction is stretched relative to the shock-contact structure, while in Figure 2(d) the situation is reversed. These results are consistent with those presented in [8].

## 4.2. Spherically symmetric dust accretion onto a black hole

In this test case we consider the simplest example of accretion onto a black hole, in which dust (gas with  $p \approx 0$ ) is accreting onto a spherically symmetric Schwarzschild black hole with mass  $M$ . As in [8] we consider the Schwarzschild metric in Eddington-Finkelstein (EF) coordinates as well as null EF (NEF) coordinates:

$$(18) \quad ds^2 = - \left(1 - \frac{2M}{r}\right) dt^2 + \frac{4M}{r} dt dr + \left(1 + \frac{2M}{r}\right) dr^2 + r^2 d\Omega^2,$$

$$(19) \quad ds^2 = - \left(1 - \frac{2M}{r}\right) dt^2 + 2 dt dr + r^2 d\Omega^2,$$

respectively, where  $r$  is the distance from the black hole,  $d\Omega^2 = d\theta^2 + \sin^2(\theta)d\phi^2$ , and  $r = 2M$  is the location of the event horizon.

The exact steady-state solutions for the boundary conditions described in [8] are

$$\rho_\infty(r) = \frac{0.195}{\sqrt{2Mr^3}}, \quad v_\infty^{1,\text{EF}}(r) = \frac{-4M^2 - \sqrt{2Mr^3}}{r^2 + 2Mr + 4M^2}, \quad v_\infty^{1,\text{NEF}}(r) = -\frac{2M}{r} - \sqrt{\frac{2M}{r}}.$$

The numerical results using the proposed residual distribution schemes are shown in Figure 3. Displayed in these plots are (a) the density as a function of distance from the black hole center, (b) numerical convergence results for the  $P^1$ ,  $P^2$ , and  $P^4$  schemes, (c)  $v^1$  in EF coordinates, and (d)  $v^1$  in null EF coordinates. The solid lines are the exact solutions and the open circles are the results using the  $P^2$  scheme with 100 elements (i.e., a total of 201 nodes). The solutions are computed for  $0.5M \leq r \leq 15M$ .

**Acknowledgments.** This work was supported in part by NSF grant DMS-0409972.

## References

- [1] R. Abgrall. Toward the ultimate conservative scheme: Following the quest. *J. Comp. Phys.*, 167, 2001.
- [2] R. Abgrall and M. Mezone. Construction of second order accurate monotone and stable residual distribution schemes for unsteady problems. *J. Comp. Phys.*, 188, 2003.
- [3] R. Abgrall and P.L. Roe. High order fluctuation schemes on triangular meshes. *J. Sci. Comp.*, 19, 2003.
- [4] Á. Csík and H. Deconinck. Space-time residual distribution schemes for hyperbolic conservation laws on unstructured linear finite elements. *Int. J. Num. Meth. Fluids*, 40, 2002.
- [5] D.S. Bale, R.J. LeVeque, S. Mitran, and J.A. Rossmannith. A wave propagation method for conservation laws and balance laws with spatially varying flux functions. *SIAM J. Sci. Comp.*, 24:955–978, 2003.
- [6] J.A. Font. Numerical hydrodynamics in general relativity. *Living Rev. Rel.*, 2000.
- [7] C.W. Misner, K.S. Thorne, and J.A. Wheeler. *Gravitation*. W.H. Freeman, San Francisco, 1973.
- [8] P. Papadopoulos and J.A. Font. Relativistic hydrodynamics on spacelike and null surfaces: formalism and computations on spherically symmetric spacetimes. *Phys. Rev. D*, 61(024015), 1999.
- [9] L. Del Zanna and N. Bucciantini. An efficient shock-capturing central-type scheme for multidimensional relativistic flows, I. Hydrodynamics. *Astron. Astrophys.*, 390:1177–1186, 2002.

JAMES A. ROSSMANITH

DEPARTMENT OF MATHEMATICS, UNIVERSITY OF WISCONSIN

480 LINCOLN DR., MADISON, WI 53706-1388

*E-mail address:* rossmani@math.wisc.edu